Proceedings of the NASA 2020

UNSGC Fellowship Symposium

May 10, 2021, Salt Lake City, UT, USA

Electromagnetic 3D printing for responsive architectures with an orthogonal magnetic field

Brian Elder, Yong Lin Kong[*]

Department of Mechanical Engineering

University of Utah

Salt Lake City, UT 84112 (USA)

**Corresponding Author's E-mail: yong.kong@utah.edu*

1. INTRODUCTION

The integration of nanomaterials with 3D printing can enable the creation of responsive architecture with highly tunable functional properties. Magnetic nanopatterning is attractive for its ability to produce untethered, high energy density actuation with a broad range of applications. For example, biocompatible materials (such as silicone rubber) can be programmed in an extrusion-based 3D printing process to create a responsive medical soft robot structure.

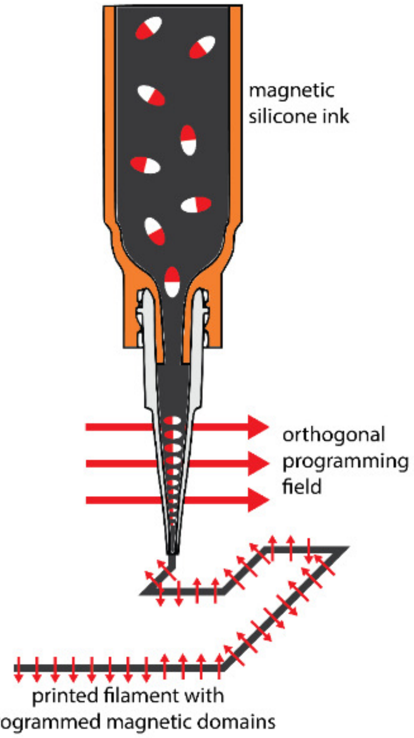

Figure 1. Illustration of the Direct Ink Writing (DIW) and magnetic programming process. Silicone ink containing suspended ferromagnetic particles is extruded through a nozzle, where it encounters an orthogonal magnetic field that aligns the magnetic particles. The ink is deposited onto the substrate, where a magnetic shield prevents further programming. The printed filament is cured, locking the programmed magnetic domains within the polymer network.

Previous works have demonstrated the use of electromagnetic coils to program magnetic remanence in a ferromagnetic medium during a 3D printing process.[1–3] For example, Kim et al.[3] demonstrated DIW with a concentric electromagnet around the nozzle to program an axial magnetic remanence in the filament. This project seeks to investigate the programming of transverse magnetic remanence during a DIW process with an orthogonal magnetic field. The outcome of this study can enable the production of ferromagnetic silicone structures with novel magnetic domain programming capability. As a first step, we will evaluate the hypothesis that the programming of transverse magnetic domains in a 3D printed filament can be achieved by applying a transverse magnetic field across the tip of a DIW nozzle.

2. MATERIALS AND METHODS

2.1 Ferromagnetic silicone ink

The 3D printed ink consists of a silicone base—a 2:1 mixture of Ecoflex 00-30 Part B (Smooth-On) and DOWSIL SE 1700 (Ellsworth). The shear-thinning property of the ink is tuned by adding fumed silica nanoparticles (amorphous, 20–30 nm, 2.72 wt%, US Research Nanomaterials). Ferromagnetism is imparted to the ink through the addition of neodymium-iron-boron (NdFeB) particles (5 µm, 20 vol%, Magnequench). Before printing, the ink is mixed with a 10 vol% SE1700 catalyst with respect to the SE1700 and magnetized by an ~2.7 T magnetic field in an impulse magnetizer.

2.2 Magnetic programming and DIW

The magnetic ink is loaded into a 3 cc syringe barrel fitted with an 840 µm plastic nozzle. The ink is extruded pneumatically with a digital pressure regulator. The conversion between pressure and extrusion rate is empirically determined immediately before each print. The syringe barrel is attached to a custom 3-axis gantry (AGS1000, Aerotech) by a custom fixture that holds the programming coil and magnetic shielding. A custom master program interfaces with the gantry and peripherals. The printing path is pre-generated via either (1) feeding a CAD model into digital slicer software to generate G-code, which is then interpreted by the master program; or (2) the master program that can generate continuous print paths for simple shapes with fewer parameters. In this paper, we will focus on leveraging method (2).

During the 3D printing process, the master program monitors the position and

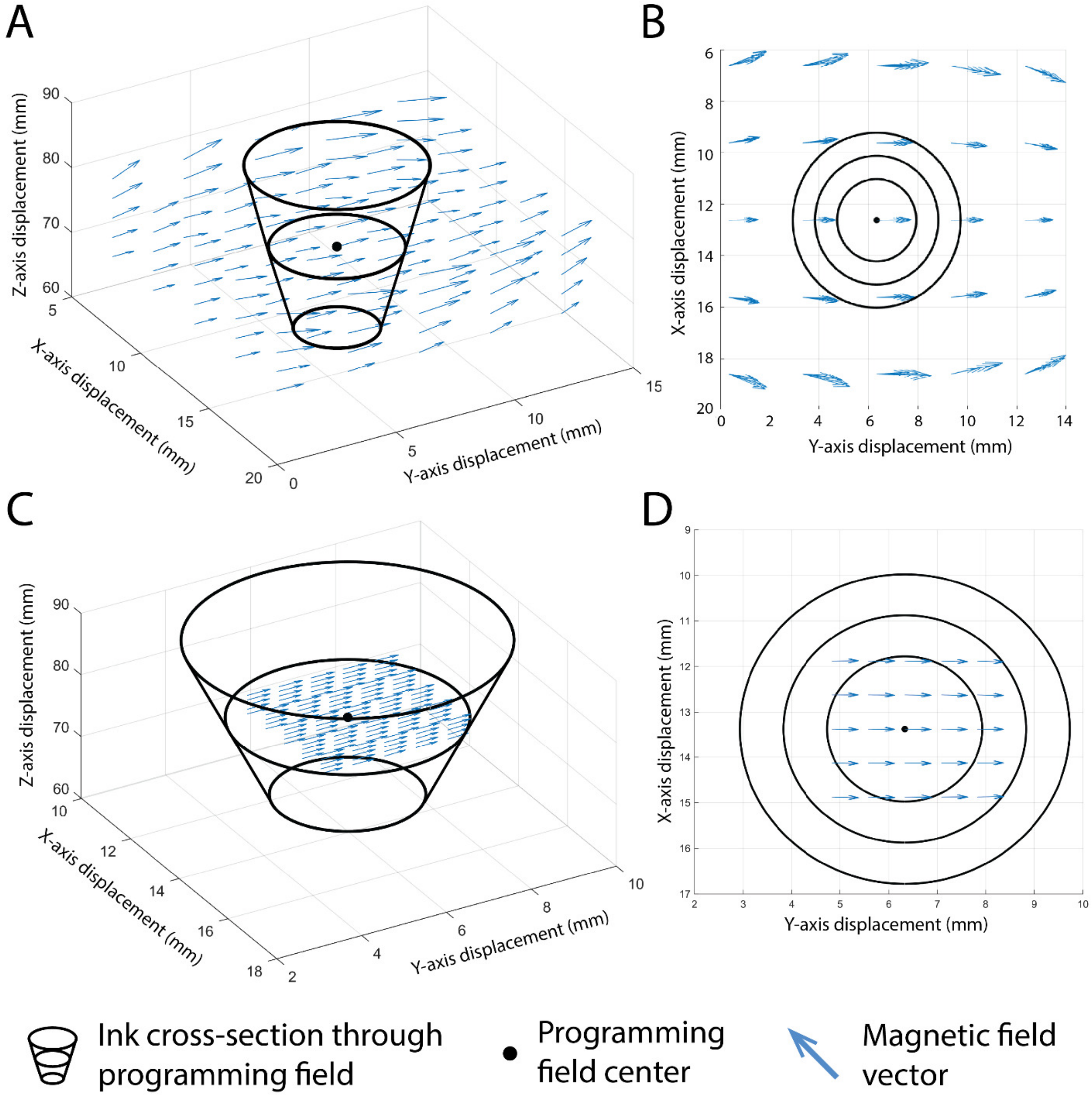

Figure 2. Magnetic field characterization of the center of the programming field. **(A)** 3D view of the magnetic flux vectors found by the coarse sweep. Data resolution is 1 mm, plotted every 3rd data point. Black circles depict the outer surface of the nozzle, with a black dot at the center of the ink extrusion path. **(B)** A top-down view reveals a uniform field at the nozzle location. **(C)** 3D view of the magnetic flux vectors found by the fine sweep. Data resolution is 0.25 mm, plotted every 3rd data point. **(D)** A top-down view confirms the uniformity of the magnetic field. The normalized means of these flux vectors are: 0.999 (SD 0.001) along the Y-axis, 0.0119 (SD 0.0129) along the X-axis, and 0.0048 (SD 0.042) along the Z-axis.

velocity of the gantry and uses this information to update the strength and direction of the magnetic field to conform to the pre-determined domain pattern. The master program communicates through a socket to a dedicated Raspberry Pi that controls the electromagnet coils and monitors temperature and current feeds.

2.3 Coil temperature monitoring

The sub-surface temperature of the coil is measured by a K-type thermocouple that is embedded halfway into the coil wrappings. This thermocouple is wired into the Raspberry Pi for continual monitoring. The master program accesses this data through the socket.

2.4 Magnetic actuation

A large permanent magnet (2 inch outer diameter, 1 inch thick, neodymium 52 grade) was used to induce shape deformation in the printed structure. For example, the magnetic field strength of ~1500 gauss can be achieved at a separation distance of ~1 inch.

2.5 Fluorescence imaging and analysis

The magnetic actuation of the printed shape is recorded via fluorescence photography. This photography technique is enabled by mixing a red fluorescent pigment (Ignite, Smooth-On) into the ink (an additional 2 wt%) before printing.

A DSLR camera captures images and videos (EOS 80D, Canon) mounted above the subject. The camera is fitted with a deep red filter (Dark Red MRC 091M, B+W) to block all but the light from the fluorescence. The subject is placed on an elevated surface to allow the large permanent magnet to be placed underneath to actuate the subject. This setup is housed in a blackout box. UV LEDs illuminate the subject (realUV, Waveform Lighting).

After capturing high-contrast, grayscale images, the images are loaded into MATLAB for analysis. We note that only a monochrome channel (in this case, red) is needed to form the image (Figure 4D). Image

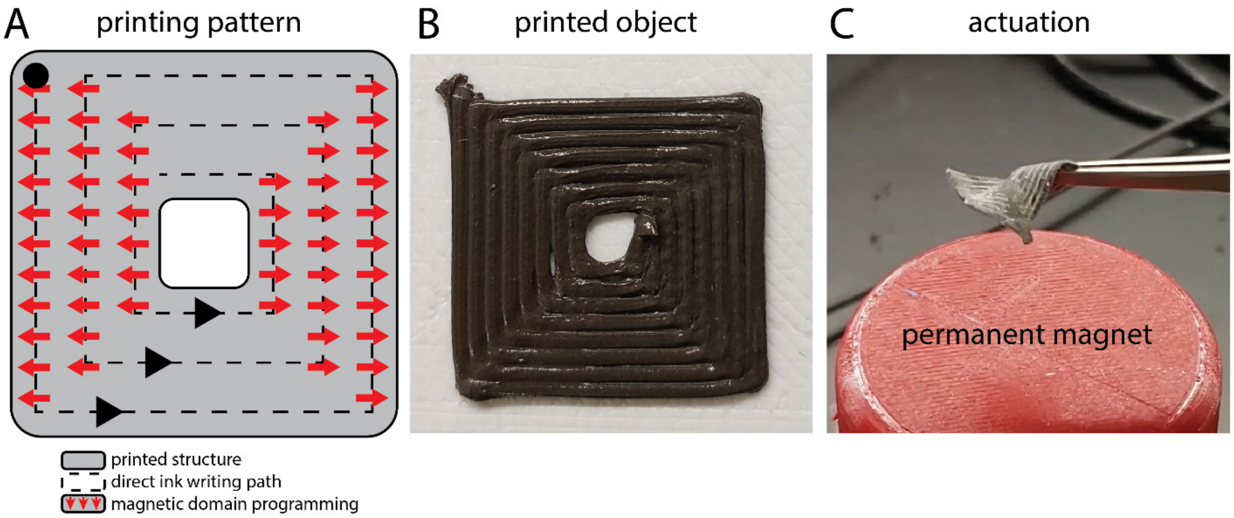

Figure 3. Domain programming, from design to functional demonstration. **(A)** A 2D structure is designed to be printed with a single, unbroken filament (dotted lines), with heterogenous, programmed magnetic domains (red arrows). The black circle indicates the starting position and the black arrows indicate the printing direction (an inward spiral). **(B)** A custom printer and electromagnetic printhead produce the structure. After printing, the silicone structure is post-cured to fix the magnetic domains. **(C)** The heterogenous magnetic domain patterning causes the structure to deform when subjected to a static magnetic field.

analysis techniques are applied to filter the image and fit a smooth curve to the shape of the subject (Figure 4E), which describes the deformation of the subject.

2.6 Magnetic field characterization

The magnetic field of the coil was mapped in a volume around the programming focal region. Two volume sweeps were performed, one in a 19x29x19 mm region with 1 mm resolution and one in a 5x5x5 mm region with a 0.25 mm resolution. The field was mapped with a custom magnetometer probe that was attached to a 3-axis gantry.

3. RESULTS AND DISCUSSION

The coils are wrapped around an iron core that concentrates the magnetic flux across the air gap on either side of the nozzle (Figure 1). To verify that the magnetic field is uniform within the volume of ink that passes through the center of the field, a custom magnetometer was used to measure the magnetic flux between the coils. The volume sweep started with a coarse sweep (1 mm resolution) to find the center of the field, followed by a finer sweep (0.25 mm resolution) centered around the approximate center of the field. The 3D quiver plots in

Figure 2 show the magnetic flux vectors found by the coarse and fine sweeps.

The normalized means of the magnetic flux vectors inside the nozzle region are 0.999 (SD 0.001) along the Y-axis, 0.0119 (SD 0.0129) along the X-axis, and 0.0048 (SD 0.042) along the Z-axis. Two factors to consider are that the coils are wound by hand without a winding spool, and during the magnetic field characterization, the coil was positioned by eye, using the gantry axes and a square. With this consideration, the minor deviations in the magnetic flux appear to be negligible for this study.

Due to physical constraints in applying a 50 mT transverse magnetic field with a lightweight, compact coil that can fit on a moving gantry, the electromagnet coil is driven at three times (18.2 A mm^{-2}) the recommended ampacity (6.0 A mm^{-2}) of electromagnet wires that are cooled by forced air.[4]

In addition to a custom-built active forced-air cooling system, the system employs reactive control by monitoring the coil's temperature, pausing the printing, and shutting down the coil if the core temperature exceeds 60 °C. The printing is resumed once the core temperature drops below 40 °C. This temperature range is well below the maximum rated temperature of the wire, 155 °C, ensuring the system's longevity.

After printing the compact spiral structure with alternating transverse magnetic domains (Figure 3A) a post-cure at 120 °C for one hour is used to fix the magnetic particles within the silicone network. After applying a vertical magnetic field underneath the table with about a one-half-inch gap, the structure shows signs of transverse magnetic domain programming.

However, as seen in Figure 3C and Figure 4C, the fidelity of the deformed structure have room for further improvement. Ideally, the responded shape should resemble a shallow “U.” In our current and future work, we will be addressing technical attributes that contribute to the deviation from the programmed shape.

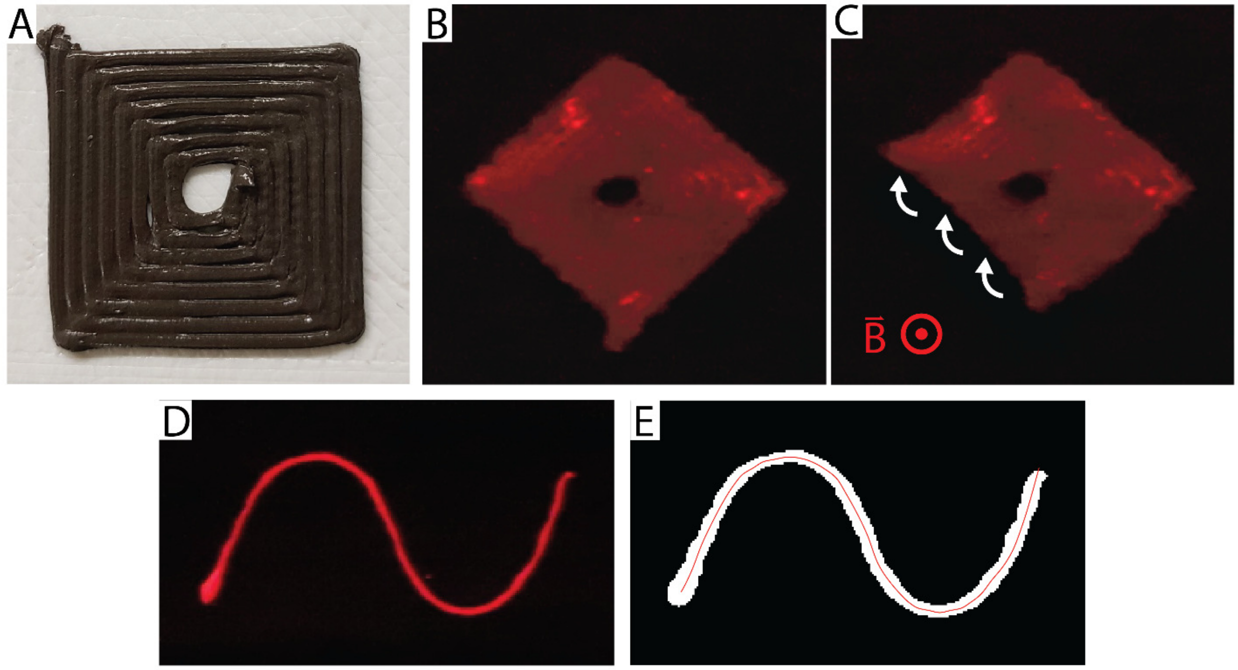

Figure 4. Fluorescence photography and image analysis. **(A)** The silicone composite ink contains a fluorescent dye that enables high contrast photography under ultraviolet (UV) light. **(B)** A 2D structure rests in the blacked-out photo studio, before the application of a magnetic field. **(C)** The application of a magnetic field causes the edges of the printed structure to curl up. **(D)** High contrast images facilitate image analysis. A single filament with a distinctive s-shaped curve is identified through image processing, and **(E)** Modified Akima interpolation is used to extract information about its curvature for future analysis.

Several primary causes have been identified, along with the strategies to address them. First, to produce the regions without programmed magnetic domains (horizontal paths in Figure 3A), the magnetic field has to be turned off during the extrusion process. However, this approach will have a small amount of residue ink in the nozzle that retains the magnetic programming it received when the field was on. In future work, we will investigate the use of a degaussing step to remove the magnetic remanence from these regions.

Second, the geometry of the coil, nozzle, and shield introduces a separation between the tip of the nozzle and the applied magnetic field. The previously programmed ink must be extruded before the newly programmed ink; this causes a delay between the moment when the magnetic field changes and when the magnetic domain changes in the printed ink. In future work, we will implement proactive measures to anticipate a change in magnetic programming and apply the change to the magnetic field ahead of time. The goal will be to queue the ink inside the nozzle with the subsequent magnetic programming so that the new section of ink begins extruding as soon as the nozzle reaches the next segment of the print.

As a next step, we will also further refine our characterization process. Specifically, we will measure the strengths and orientations of the magnetic domains of the printed parts by obtaining samples with a biopsy punch and analyzing the magnetic remanence in a spinner magnetometer. This will provide a map of the magnetic domains with a resolution of 1.5 mm.

4. CONCLUSION

Electromagnetic DIW is a versatile technique that is capable of selectively programming magnetic domains in a 3D printed construct. Here, we have demonstrated the magnetic patterning in the transverse direction of the raster pattern. The highly versatile setup also enables an exciting opportunity to develop previously unachievable complex magnetic programming capability that can ultimately enable a broad range of exciting advanced manufacturing capability for the space mission.

5. REFERENCES

[1] J. J. Martin, B. E. Fiore, R. M. Erb, *Nat. Commun.* **2015**, *6*, 8641.

[2] D. Kokkinis, M. Schaffner, A. R. Studart, *Nat. Commun.* **2015**, *6*, 8643.

[3] Y. Kim, H. Yuk, R. Zhao, S. A. Chester, X. Zhao, *Nature* **2018**, *558*, 274.

[4] J. J. Abbott, *Rev. Sci. Instrum.* **2015**, *86*, 1.